Condensed Matter Physics for Non-Destructive 100 T Magnets

Boebinger, G.S., Lucent Technologies and LANL
Brazovskii, S., Landau Institute
Campbell, L.J., NHMFL/LANL

This work[1] surveyed condensed matter research topics that can benefit from the expected availability within the next few years of non-destructive 100 T magnets having 10 ms pulse widths.[2] A related and largely complementary survey article appeared recently in *Physics Today*.[3] A bibliography of over 70 references was compiled.

The six broad areas of condensed matter physics that were found most promising to study in 100 T fields are sketched below.

1. *Basics of High Magnetic Field (HMF) Interaction with Condensed Matter*
   Orbital states: confine, localize, quantize, and break continuous degeneracy.
   Spin states: lift discrete degeneracy, decouple spins, and break singlet correlations.
   Interplay of orbital and spin HMF effects: inhomogeneous Larkin-Ovchinnikov-Fulde-Ferrell state in superconductors near the Pauli limit and skyrmions in the quantum Hall effect (QHE).

2. *Layered Systems*
   Orbital effects in 2D systems where all degrees of freedom are effected by the HMF: extraordinary new opportunities in semiconducting technology; surprises of the QHE; composite fermions; Wigner crystals.
   Reduced dimensionality also in layered systems: High-Tc superconductors and organic superconductors.

3. *Metals and SDWs*
   BEDT family of organic superconductors.
   TMTSF Bechgaard salts (first organic superconductors).

4. *High-Tc Superconductors*
   HMFs used to suppress superconducting state to reveal normal state.
   "Super-clean" regime: flux-flow Hall angle approaches $\pm\pi/2$.
   Separate relaxation times: different scattering times for transport and Hall resistivities.
   Quantum oscillations, Fermi surface via de Haas-van Alphen, re-entrant superconductivity.
   Destroy inter-plane Josephson coupling to recover a virgin single-plane contribution to pairing.

5. *Electronic Correlations in Quantized Landau*
   Levels in 3D Systems
   Semimetals
   Narrow gap- and doped semiconductors.
   Semiconductors.

6. *Real Space Cooper Pairs, Bipolarons*
   Candidate materials for bipolarons.
   HMFs can prove the existence of real space pairs by breaking them into separate but still dressed electrons (polarons).

References:

1 Boebinger, G.S., *et al*., to appear in Physica B, 1998.
2 Campbell, L.J., *et al*, Physica B, 211, 52 (1995); Askenazy, S., Physica B, 216, 221 (1996).
3 Boebinger, G.S., Physics Today, 49 #6, 36 (1996).

Magnetization and de Haas-van Alphen Measurements to 50 T on UGa_3

Cornelius, A.L., LANL
Arko, A.J., LANL
Sarrao, J.L., LANL
Thompson, J.D., LANL
Harrison, N., NHMFL/LANL

We have performed magnetization and de Haas-van Alphen (dHvA) measurements in pulsed fields to 50 T on the antiferromagnet UGa_3. The measurements were performed along the (100) axis of the cubic crystal. The measured electronic specific heat coefficient of UGa_3 is 52 mJ/mol K^2. At the lowest temperature measured (0.43 K) a magnetic transition at an applied magnetic field of B_M = 13 T, as seen in Figure 1, occurs. When the signal is plotted versus the inverse field, one observes oscillations in the signal with a frequency that is directly proportional to an extremal area of the Fermi surface; this is the dHvA effect.

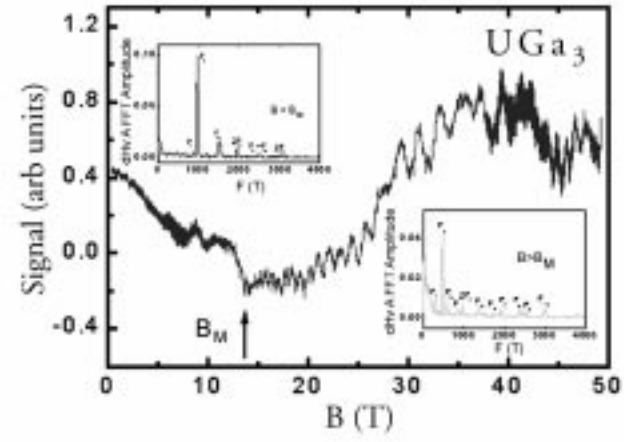

Figure 1. The measured signal versus applied pulsed magnetic field for UGa_3 along the (100) axis at 0.43 K. The insets are fast Fourier transforms of the de Haas-van Alphen signal measured above and below the magnetic transition at B_M = 13 T.

In the insets of Figure 1, there are plots of the fast Fourier transform (fft) of the signal versus inverse field for Region 1 ($B < B_M$) and Region 2 ($B > B_M$). From these plots, we observe three frequencies in Region 1 that have masses between 0.6-1.9 m_0. In Region 2, we observe 10 frequencies with masses between 0.8-5.0 m_0. Due to the fact that there is no overlap in the observed frequencies in Region 1 and Region 2, we conclude that a major reconstruction of the Fermi surface occurs at the magnetic transition at 13 T in UGa_3.

Materials for Millikelvin Thermometry in Magnetic Fields

Frederick, L., UF, Physics
Ihas, G.G., UF, Physics

Most thermometric materials are also magnetic-field sensitive (except capacitors, which must be calibrated on each cool-down). A significant body of work[1] exists in the search for a material that can be a reproducible thermometer, from cool-down to cool-down, useable in a magnetic field, and which does not need to be individually calibrated. That is, sample-to-sample calibration is sufficiently similar.

The magnetoresistance of two types of commercial thermometers, one Cernox[2] and four ruthenium

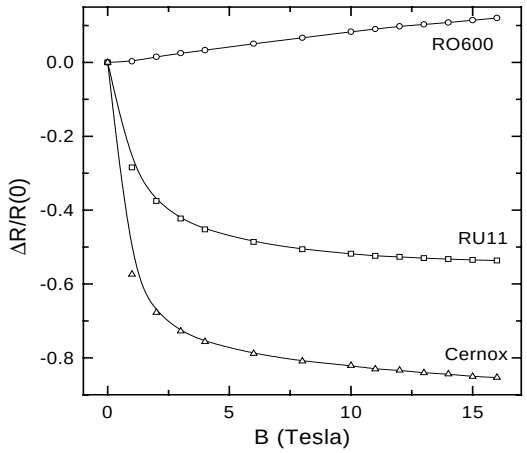

Figure 1. The change in the resistance relative to the zero field resistance for all three types of samples at 200 mK. The two RuO_2 samples have very different field dependences (a preparation dependence). Large magnetoresistance of Cernox and RU11 make them less suitable for field use.

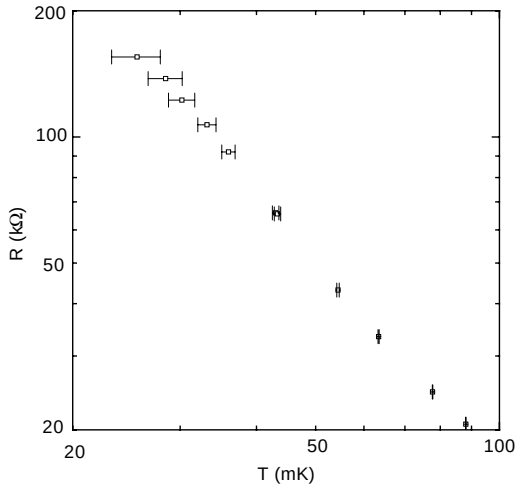

Figure 2. Variation in temperature calibration for 16 randomly picked RO600 sensors at zero field. The fit with statistical errors is:

$$Log(R) = 9.631 - 4.37697\,Log(T) + \\ +1.00025\,Log(T)^2 - 0.07915\,Log(T)^3$$

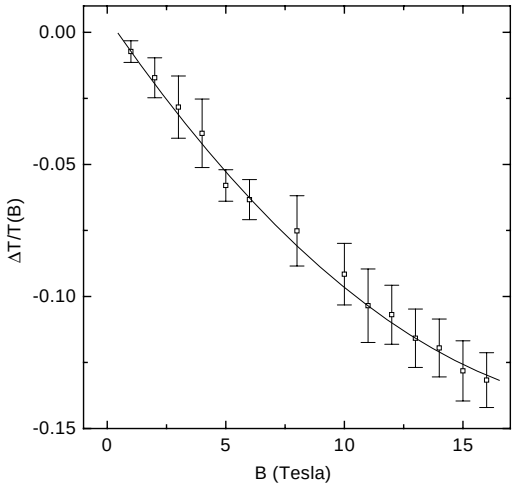

Figure 3. Relative difference of apparent temperature and the actual temperature for all four RO600s from 50 mK to 4.2 K:

$$\frac{T(0)}{T(B)} = (0.99441 + 0.01314\,B - 2.92526 \cdot 10^{-4}\,B^2)$$

oxide RO600[3] were investigated, along with a homemade RuO_2 sample (RU11)[4] (see Figures 1, 2, and 3). They were mounted in the mixing chamber of SCM-1 (T < 750 mK) and on SCM-2 (T > 750 mK) at the NHMFL. Measurements were made in thermal and field equilibrium.

The reproducibility of calibration among the various RO600 sensors indicates that they may be useful in many experiments without the need for individual calibration, using only the equations given here.

References:

1 See references in: Uhlig, K., Cryo. 35, 525.
2 Lakeshore Cryotronics, Westerville, OH.
3 Scientific Instr., West Palm Beach, FL.
4 Kim, J.S., University of Florida.

In Situ Electrical Characterization of Thin Films During Growth

Hebard, A.F., UF, Physics/NHMFL
Arnason, S.B., UF, Physics/NHMFL

It has long been recognized that ultrathin metallic films can have electronic transport properties that are significantly different than their thicker bulk-like counterparts. We are presently using *in situ* monitoring of film resistance during film growth to elucidate and understand these differences. By correlating these measurements with film thickness and deposition conditions, new phenomenon have been revealed that delineate in unexpected ways the crossover between the two-dimensional regime where the effects of surfaces and interfaces dominate, and the three-dimensional regime where the bulk properties of the material being deposited become manifest.

By way of illustration we have performed a detailed study of the transport and magnetotransport in thin silver films. Distinct functional forms of the thickness-dependent resistivity identify three separate stages of film growth: an initial nucleation and growth of isolated metal islands; growth and coalescence of these islands into a continuous network of conducting paths; and finally, an isotropic and homogeneous medium of well-connected microscopic grains. By monitoring the resistance during the growth process, we can controllably arrest film growth to produce stable films having reproducible temperature-dependent transport properties. The temperature-dependent

resistivities in the intermediate coalescence regime exhibit all of the signs of "bad metal" behavior, i.e., an anomalous high resistivity scale, strong metallic temperature dependence of the resistivity, and lack of resistive saturation. The scaling collapse of all of the data for a variety of films with different thickness onto a single curve implies that a geometrical correction (as large as a factor of 1000) must be used to take into account the effect of tortuous conduction paths with extremely thin cross sections. The most dramatic effect of this microstructure appears in the magnetoresistance (Figure 1), which has a quadratic dependence on magnetic field with a classical temperature dependence (figure inset) but a *negative* sign. Our understanding of these data is based on the recognition that transport is dominated by electron flow in narrow tortuous channels having a typical width on the order of the bulk transport scattering length. In this channel configuration much of the resistance is due to diffusive scattering at the boundaries with a backscattered component, which is suppressed because of the tortuous conduction paths. Extreme geometry corrections rather than exotic physics has thus been shown to be responsible for an unusual magnetoresistance effect in a metal masquerading as a "bad metal" but having "good-metal" components.

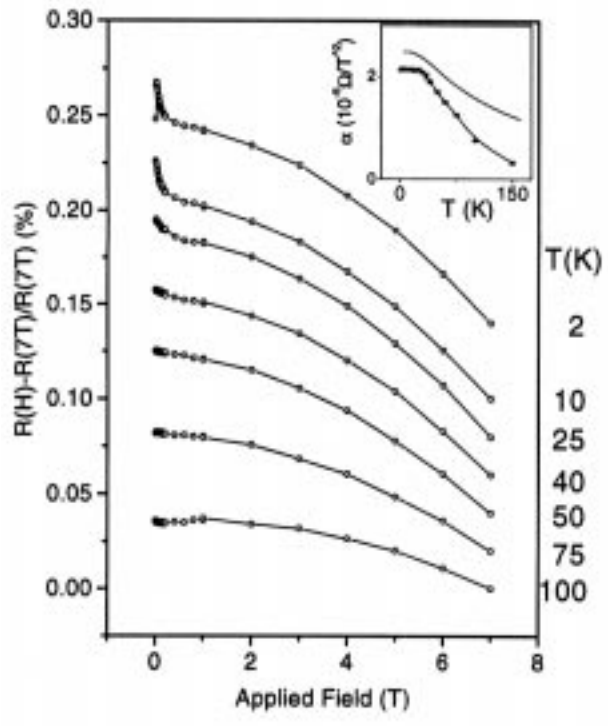

Figure 1. Magnetoresistance at the indicated temperatures. The inset shows the temperature dependence of the coefficient extracted by fitting the high field data to a parabola.

Grain Boundary Motion in Bismuth-Bicrystals

Molodov, D.A., Institute of Metallurgy and Metal Physics, RWTH Aachen, Germany
Gottstein, G., Institute of Metallurgy and Metal Physics
Heringhaus, F., NHMFL
Shvindlerman, L.S., Institute of Solid State Physics, Russian Academy of Sciences

In two series of experiments in March and October 1997, we measured the grain boundary motion in Bi-bicrystals. The driving force, *p*, for grain boundary motion (1) in these experiments was provided by a magnetic field due to the strong magnetic anisotropy of bismuth.

$$p = \mu_0 \frac{\Delta\chi}{2} H^2(\cos^2\theta_1 - \cos^2\theta_2) \qquad (1)$$

θ_1 and θ_2 are the angles between the direction of the magnetic field and the trigonal axes in both grains of the Bi-bicrystal, $\Delta\chi$ is the difference of susceptibilities parallel and perpendicular to the trigonal axis, and H is the strength of the field. For the first time a defined planar grain boundary in a specially grown bicrystal was moved by means of a magnetic driving force. To prove that boundary motion is caused exclusively by the magnetic driving force, the experiment was carried out in two different ways. By changing the position of the bicrystal with regard to the applied magnetic field the direction of the driving force was inverted, and, as expected, boundary motion in the opposite direction was observed.

The mobility of 90°<112> tilt symmetrical and asymmetrical boundaries was measured, and the dependence of grain boundary mobility on temperature and driving force was investigated. It was found that the migration parameters (activation

enthalpy, Q, and mobility preexponential factor, m_o) for the symmetric boundary (Q=0.57 eV, m_o=0.67 $m^4/J{\cdot}s$) drastically differs from the migration parameters for the asymmetrical boundary ($Q_{||}$=3.38 eV, $m_{o||}=2.51{\cdot}10^{26}$ $m^4/J{\cdot}s$, $Q_{\perp}$=3.79 eV, $m_{o\perp}=1.26{\cdot}10^{30}$ $m^4/J{\cdot}s$). The symmetrical boundary possesses a higher mobility than the asymmetrical boundary in the entire investigated temperature range up to the melting point of Bi (Figure 1). The mobility parameters for the asymmetrical boundary were found to be distinctly different in opposite directions, such that the boundary is less mobile if the c-axis in the growing grain is perpendicular to the direction of motion; and it is more mobile if the trigonal c-axis in the growing grain is parallel to the direction of motion. This result provides evidence that Bi possesses an anisotropy of grain growth perpendicular and parallel to the trigonal axis.

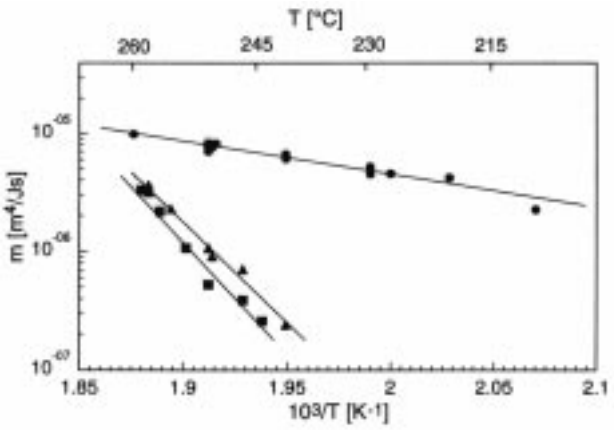

Figure 1. Temperature dependence of the mobility of 90°<112> symmetrical (●) and asymmetrical (▲,■) tilt boundaries in Bi-bicrystals: ▲ and■ - c-axis in the growing grain is || and ⊥ to the growth direction, respectively.

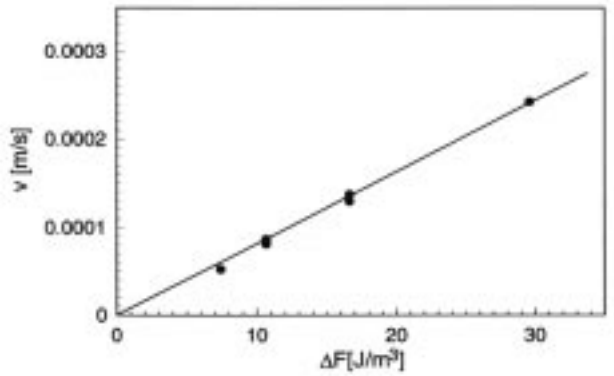

Figure 2. Dependence of the velocity of 90°<112> symmetrical tilt boundary on the magnetic driving force.

The measurements of the boundary migration in different magnetic fields revealed that even in the region of very small driving forces the boundary velocity changes linearly with driving force (Figure 2).

Quantum Properties of Electrons in Spatially Varying Magnetic Fields

Schrieffer, J.R., NHMFL/FSU, Physics
Hu, J., NHMFL

We have studied the electronic structure of electrons moving in spatially varying magnetic fields. The case of a magnetic field varying linearly with position and that of a uniform field with a periodic field have been investigated with the inclusion of spin. The DC conductivity in the relaxation time approximation $\sigma(o)$ has been calculated for the linearly varying magnetic field and the optical conductivity for the periodic field case. We find novel oscillatory behavior of $\sigma(o)$ in the linear field case. For the oscillatory magnetic field, the Landau levels for the uniform field go over energy bands for the oscillatory field.

Absorption Spectra of C_{60} in High Magnetic Fields

Srdanov, V.I., Univ. of California at Santa Barbara, Chemistry
Lewis, W., Bechtel
Marshall, B., Bechtel
Kim, Y., NHMFL/LANL
Campbell, L.J., NHMFL/LANL

Prompted by reports from a Russian group regarding unexpected behavior of C_{60} in high magnetic fields, researchers from UC Santa Barbara, Bechtel in Nevada, and NHMFL-LANL initiated a joint project. The efforts were focused on detecting changes in absorption spectra of a thin film of C_{60} (Figure 1) in ultrahigh magnetic fields generated by the Dirac II series. The project first required development of a

method for epitaxial growth of a thin film of C_{60} on the tip of an optical fiber. In addition, an optical set-up—fast and sensitive enough to record transient absorption spectra of C_{60} during several microseconds of the DIRAC explosion—had to be designed and optimized.

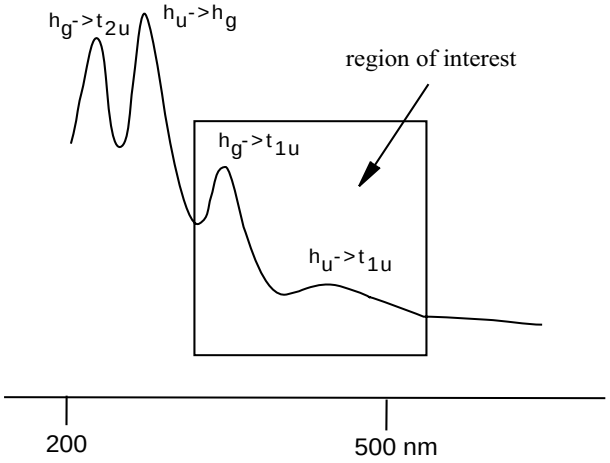

Figure 1. Absorption spectrum of C_{60}.

After successful preparations, which included practice "shots" on the 50 T magnet at Los Alamos, two Dirac experiments involving thin films of C_{60} went well and a portion of the C_{60} spectrum in the high magnetic field has been recorded. A large bulk of numerical data is being processed at this point and will be correlated with the magnetic susceptibility measurements on C_{60} obtained under the same experimental conditions by the Russian team.

Magnetoresistance in $CeMn_2Ge_{2-x}Si_x$ Compounds

Torikachvili, M.S., San Diego State Univ., Physics
Bud'ko, S.L., Centro Brasileiro de Pesquisas Físicas (CBPF), Brazil
Fontes, M.B., CBPF
Baggio-Saitovitch, E., CBPF
Lacerda, A.H., NHMFL/LANL

We studied the transport and magnetotransport properties of $CeMn_2Ge_{2-x}Si_x$ compounds, with x = 0.8 - 1.2, in the temperature T range from 2 K to 300 K, in magnetic fields to 18 T. Neutron scattering experiments[1] in $CeMn_2Ge_2$ and $CeMn_2Si_2$ suggest that (1) $CeMn_2Ge_2$ first becomes a collinear antiferromagnet (AF) at $T_N \approx 415$ K, and then develops a conical structure with a ferromagnetic (FM) component along the c-axis below $T_c \approx 318$ K; and (2) $CeMn_2Si_2$ becomes AF at $T_N \approx 380$ K. At intermediate concentrations a cross-over from AF to FM is expected.[2] We found that the T dependence of the electrical resistivity ρ varies greatly in the concentration range x = 0.8 - 1.2, suggesting a complex magnetic behavior. The ρ vs. T curve for $CeMn_2Ge_{0.8}Si_{1.2}$ displays a minimum at 167 K, a maximum at 74 K and then a sharp drop below 25 K, which is reminiscent of drops seen in FM materials due to the suppression of spin-flip scattering. As more Ge is substituted for Si both the T of the minimum and maximum are shifted towards lower T, while the sharp drop of ρ at low T merges with the peak in ρ vs. T. At intermediate T between the maximum and minimum in ρ vs. T the magnetoresistance (MR) is very small for the compounds with x = 0.8, and 0.9, and negative for x = 1.0, 1.1, and 1.2. The behavior of the MR at low T differs greatly between the compounds, also indicating complex magnetic behavior.

References:

1 Fernandez-Baca, J.A., *et al.*, J. Appl. Phys., 79, 5398 (1996).
2 Hill, P., *et al.*, J. Appl. Phys., 73, 5683 (1993).

De Haas-van Alphen Measurements in Pd and Concentrated Binary Alloys

Vuillemin, J.J., Univ. of Arizona, Physics
Goodrich, R.G., Louisiana State Univ., Physics
Harrison, N., NHMFL
Wolters, C., NHMFL
Hall, D., LSU, Physics

The dHvA effect in Pd was studied with the field along [100] to obtain detailed information about its electronic structure. An important new dHvA frequency of 73.5 kT was found with an effective mass m = 12.5 using the NHMFL Pulsed Field

Facility at Los Alamos. This frequency corresponds to the largest orbit on the open hole sheet of the Fermi surface (FS) predicted by band theory.

Spin splitting of Landau levels in Pd was determined from the dHvA harmonic content. The first harmonic electron signal passes through a node near 50 T. At higher fields, there is a strong second harmonic component (Figure 1a) that is absent slightly below 50 T (Figure 1b). This suggests that the g-factor changes in this field range.

dHvA measurements were also made in concentrated Au(Ag) alloys using the cantilever method in the 33 T resistive magnet system at the NHMFL in Tallahassee, Florida. Figure 2a shows the dHvA neck oscillation in an 22% Ag alloy and Figure 2b shows the dHvA frequency as a function of Ag concentration.

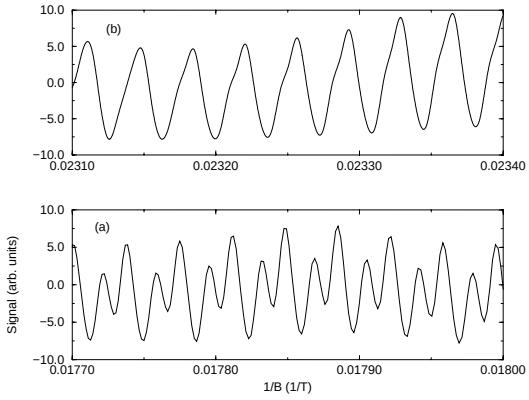

Figure 1. The dHvA signal in Pd with T = 2 K.

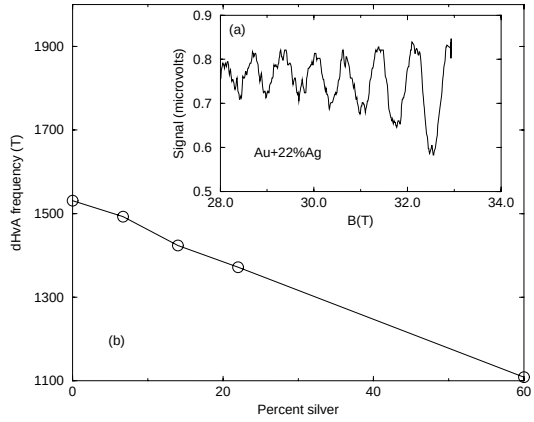

Figure 2. The dHvA signal in Au (Ag) with the field along [111] and T = 1.5 K.

Anisotropy Study of Sonoluminescence Under Magnetic Fields

Young, J.B., Univ. of Chicago, Physics and James Franck Institute
Cho, H., Univ. of Chicago, Physics and James Franck Institute
Kang, W., Univ. of Chicago, Physics and James Franck Institute

A small bubble of gas, suspended at a velocity node of an acoustic cavity, can emit an extremely short pulse of light when driven by sufficiently intense sound field.[1,2] This phenomenon, called sonoluminescence (SL), represents a most singular energy conversion process where the externally applied sound energy is converted to light. The emitted light exhibits rather interesting properties such as extremely short pulse length (~ 100ps),[3] spectrum that appears to be centered at UV or soft X-ray energies,[4] and a high degree of synchronicity between successive pulses.[3] While the actual mechanism of light emission has remained elusive, circumstantial evidence suggests that extremely high temperatures (as high as 100,000 K) may be attained at the center of the bubble.

Studies of sonoluminescence in magnetic fields up to 20 T have revealed a striking magnetic field dependence.[5] The intensity of emitted light is suppressed under increasing magnetic fields and vanishes above threshold magnetic field that depends on the applied sound pressure. Further increase in the magnetic field leads to the destruction of the bubble through dissolution. At a constant magnetic field, the light intensity is found to increase roughly linearly with increasing sound pressure until the bubble disappears above a cut-off pressure which depends on the strength of the magnetic field.

The cut-off pressure is found to approximately double between 0 T and 20 T. Further study of

the SL bubble through the measurement of the phase of the emitted radiation relative to acoustic drive shows a large increase in phase under magnetic fields.[6] These results suggest that the bubble grows significantly in size and that there may be a substantial modification of bubble dynamics under magnetic field. The origin of the observed effects may occur as a consequence of magnetic field-induced anisotropies in the SL bubble.

References:

1 Barber, B.P., *et al*., Nature (London), 352, 318 (1991).
2 Gaitan, D.F., *et al*., J. Acoust. Soc. Am., 91, 3166 (1992).
3 Barber, B.P., *et al*., Phys. Rev. Lett., 69, 3839 (1992).
4 Hiller, R., *et al*., Phys. Rev. Lett., 69, 1182 (1992).
5 Young, J.B., *et al*., Phys. Rev. Lett., 77, 4816 (1996).
6 Young, J.B., *et al*, unpublished.